Biosensors and Bioelectronics 70 (2015) 61–68

Contents lists available at ScienceDirect

Biosensors and Bioelectronics

journal homepage: www.elsevier.com/locate/bios

Giant magnetoresistive-based biosensing probe station system for multiplex protein assays

Yi Wang [1], Wei Wang [1], Lina Yu, Liang Tu, Yinglong Feng, Todd Klein, Jian-Ping Wang *

Department of Electrical and Computer Engineering, University of Minnesota, Minneapolis, MN 55455, USA

ARTICLE INFO

Article history:
Received 2 November 2014
Received in revised form
19 January 2015
Accepted 4 March 2015
Available online 10 March 2015

Keywords:
Magnetic biosensor
Giant magnetoresistance
Biomarker detection
Multiplex
Point-of-care
Probe station

ABSTRACT

In this study, a sensitive immune-biosensing system capable of multiplexed, real-time electrical readout was developed based on giant magnetoresistive (GMR) sensor array to detect a panel of protein biomarkers simultaneously. PAPP-A, PCSK9, and ST2 have been regarded as promising candidate biomarkers for cardiovascular diseases. Early detection of multiple biomarkers for a disease could enable accurate prediction of a disease risk. 64 nano-size GMR sensors were assembled onto one 16 mm × 16 mm chip with a reaction well, and they could work independently and be monitored simultaneously. A detect limit of 40 pg/mL for ST2 antigen had been achieved, and the dynamic ranges for the three proteins detection were up to four orders of magnitude. The GMR sensing platform was also selective enough to be directly used in serum samples. In addition, a lab-based probe station has been designed to implement quick lab-on-a-chip experiments instead of wire bonding. It has a potential application in clinical biomarkers identification and screening, and can be extended to fit other biosensing schemes.

1. Introduction

In vitro diagnostics plays a key role in modern healthcare and is of great importance due to the increasing need for more effective and efficient personalized healthcare. In biomedical diagnosis, protein biomarkers show prominent promise in early detection of many diseases, such as cancer, cardiovascular and infectious diseases (Zhang et al., 2004; Vasan, 2006; Simon et al., 2004). Furthermore, the quantitative analysis of protein biomarkers also helps to make the rational treatment plan in disease development through screening as well as staging, metastasis evaluation, and assessment of treatment efficacy (Ivanov et al., 2009; Madu and Lu, 2010). Usually, a single protein biomarker is not qualified to specifically and sensitively identify the disease at an early stage. Therefore, the use of a panel of biomarkers to identify at-risk individuals with adequate confidence is intensively required for early diagnosis. Additionally, regular and frequent screening events are usually recommended in the progresses of disease diagnosis and treatment. Currently most of diagnostic tests are carried out in centralized labs hosting a great variety of analytical instruments, and complicated and professional procedures are also required. These predicaments call for the development of new techniques which are portable, and cost-effective, and also provide rapid, highly sensitive and multiplex test results. For most lab-on-a-chip platforms, wire bonding is a common method but its fragility requires high operation standard of users and transport protection, which is also critical for lab-based tests.

To date, two predominant modes have been developed for a multiplex immunoassay. The first was the multi-labeling method in which different labels tagged to different antibodies or antigens that corresponded to the analytes. A dual-label immunoassay method for the simultaneous determination of α-fetoprotein (AFP) and free β-human chorionic gonadotropin (hCGβ) using two rare earth elemental tags has been developed (Wilson and Nie, 2006). Multicolored quantum dots were also used to detect multiple cancer biomarkers in serum (Hu et al., 2009). The second method was using spatial immunoreaction localization to discriminate between different analytes. Various kinds of specific biomolecules were immobilized on 2D solid surfaces such as glass slide, silicon nanowire, and gold, etc. (Roda et al., 2011; Zheng et al., 2005; Qureshi et al., 2010). This spotted microassay allowed massively parallel analysis of multiple biomarkers, and the detection of signals from different immunoreaction zones could be achieved by using fluorescent, magnetic, chemiluminescent, electrical, electrochemical, and surface plasmon resonance measurements (Roda et al., 2011; Zheng et al., 2005; Fragoso et al., 2011; Murphy et al., 2008; Homola et al., 2005). Among these technologies, bio chip-based assay using giant magnetoresistive (GMR) sensors and magnetic labels have emerged recently (Gordon and Michel, 2012; Baselt et al., 1998; Graham et al., 2004; Schotter et al., 2004; Srinivasan et al., 2009; Rife et al., 2003; Zhi et al., 2012). GMR sensor

* Corresponding author. Fax: +1 612 625-4583.
E-mail address: jpwang@umn.edu (J.-P. Wang).
[1] These authors contributed equally to this work

http://dx.doi.org/10.1016/j.bios.2015.03.011
0956-5663/

has been widely and successfully used in hard drive head since the late 1990s (Tsang et al., 1998; Parkin et al., 2003). In biomolecular diagnostics, GMR bio-sensing technology has the advantages of low cost, high possibility in portability, high sensitivity, and real-time signal readout. The fabrication of GMR biosensor are carried out by a complementary metal-oxide-semiconductor (CMOS) compatible top-down approach, and its further integration and miniaturization is also compatible with the System on Chip technology. Therefore, it has great potential for eventually realizing POC and portability for GMR biosensor in the near future. The detection signal for GMR bio-sensing stems from magnetic excitation of magnetic labels on sensor surface. In contrast to colorimetric methods, the background signal is extremely low due to the fact that the magnetic background of biological fluids is almost negligible. Since the application of GMR technology in molecular diagnostics was proposed (Baselt et al., 1998), GMR biosensor had so far been used for the detection of protein biomarkers (Gordon and Michel, 2012; Srinivasan et al., 2009; Tsang et al., 1998; Li et al., 2010), nucleic acids (Zhi et al., 2012; Martins et al., 2009; Mulvaney et al., 2007), and metal ion (Wang et al., 2014a;2014b). Remarkably, GMR-based sensing platform that was matrix-insensitive (serum, urine, cell lysate or saliva) and capable of monitoring the kinetics of protein interactions had been also developed (Gaster et al., 2009, 2011). High-moment nanoparticles were proposed and confirmed to further enhance the signal level of GMR biosensing system (Srinivasan et al., 2009; Jing et al., 2009). These powerful capabilities would enable GMR biosensor to be a versatile and strong contender in molecular diagnostics.

Cardiovascular disease is a significant public health threat and the leading cause of death worldwide (Tarzami, 2011; Chan et al., 2011). Early diagnostic and prevention are public health priorities. The alteration of cardiovascular biomarkers at the molecular level may suggest the presence of an underlying disease state (Vasan, 2006). Among cardiovascular biomarkers, pregnancy-associated plasma protein A (PAPP-A) (Bonaca et al., 2012; Li et al., 2012), proprotein convertase subtilisin/kexin type 9 (PCSK9) (Cui et al., 2010; Huijgen et al., 2012), and suppression of tumorigenicity 2 (ST2) (Weinberg et al., 2003; Rehman et al., 2008) have been investigated and they are regarded as promising candidate biomarkers. Especially ST2, an interleukin-1 receptor family member, has strong clinical and biochemical correlates in patients with acute heart failure. The Presage ST2 Assay was approved by US FDA in December 2011, and this commercially available assay kit is indicated to be used as an aid in assessing the prognosis of patients diagnosed with chronic heart failure.

In the present study, the three protein biomarkers of PAPP-A, PCSK9 and ST2 were chosen as model protein analytes, which were simultaneously and sensitively analysed by a lab-based GMR biosensing probe sensing platform. It is also noteworthy that the proposed system with wide dynamic ranges and low background noise can also be used for other kinds of multiplexed immunoassay panels, e.g., cancer or infectious disease detection.

2. Materials and methods

2.1. Materials

3-aminopropyltriethoxy silane (APTES, 99%), glutaraldehyde (Glu, Grade II) solution, bovine serum albumin (BSA), and tween 20 were purchased from Sigma-Aldrich. Phosphate buffered saline (PBS, pH 7.4, 1 ×), and streptavidin-AF555 (2 mg/mL in PBS, pH 7.2) were purchased from Invitrogen, USA. Monoclonal rat anti-PAPP-A (catalog number MAB2487), monoclonal rat anti-PCSK9 (catalog number MAB3888), and polyclonal goat anti-ST2 (catalog number AF523) were used as capture antibody in the assay. Polyclonal goat anti-PAPP-A (catalog number BAF2487), polyclonal sheep anti-PCSK9 (catalog number BAF3888), and polyclonal goat anti-ST2 (catalog number BAF523) were used as detection antibody, and all the detection antibodies had been biotinylated. Besides these capture and detection antibodies, recombinant human PAPP-A (catalog number LUCA2487), PCSK9 (catalog number LUCA3888) and ST2 (catalog number LUCA523) antigens were also obtained from R&D Systems, Inc., USA.

2.2. GMR sensor and chip fabrication

A multi-layer GMR film structure was designed as Ta/NiFe [20]/CoFe [10]/Cu [33]/CoFe [25]/IrMn [80]/Ta (all units in angstroms) and deposited on 4-inch wafers in a six-target Shamrock sputter (Fig. S1). The anti-ferromagnetic IrMn layer is used to pin the fixed magnetic CoFe layer, and the free layer consists of CoFe and NiFe bi-layers. The wafers were pre-coated with around 1000 Å SiO_2 isolation layer through wet oxidation. By using photolithography technique and dry etching, GMR strips in the desired shape were remained. One strip has a dimension of about 120 μm × 750 nm. The gaps (1 μm in width) between the adjacent strips were filled with 100-nm thick SiO_2 film in Varian evaporator system. 50 strips connected by gold electrodes in series and parallel work as one GMR sensor. 8 × 8 sensor array is designed in one chip (Fig. 1(a)) which is about 16 mm × 16 mm, and 21 available chips are manufactured from each 4-inch wafer. The surface of chip was coated with 20 nm Al_2O_3 and 20 nm SiO_2 for the surface protection and functionalization. All chips were annealed at 200 °C for 1 h under 4.5 kOe magnetic field to align the magnetization orientation of the pinned layer. As shown in Fig. 1(b), a round reaction well was attached on the chip.

2.3. Surface functionalization

GMR chip surface was modified by 3-aminopropyltriethoxy silane (APTES) and glutaraldehyde (Glu) (Wang et al., 2013). In detail, the chip was immersed in acetone under sonication for 10 min, then transferred into isopropanol and ultrasonically treated for another 10 min. After being washed with water and dried with nitrogen gas, the chip was soaked in 10 mL of 0.5% APTES solution (in toluene) for 15 min at room temperature, followed by being thoroughly rinsed with acetone and deionized (DI) water to remove absorbed APTES. The APTES modified chip was further placed in 10 mL of 5% Glu solution that prepared by diluting 25% Glu in PBS buffer (1 × , pH 7.4). The solution was gently shaken for 5 h at room temperature, and then the chip was washed with DI water and dried by nitrogen gas. After APTES-Glu modification, the chip was stored in desiccated environment if it was not used for proteins immobilization immediately.

2.4. Multiplex protein immunoassay

For multiplex experiments with three different proteins on one chip, BSA (10 mg/mL) and three capture antibodies (PAPP-A, PCSK9, and ST2 at 500 μg/mL) were robotically spotted onto individual sensors (Fig. S2). Each droplet has about 1.6 nL in volume. It shows that the protein solutions had exactly cover the sensors, thus the proteins could be immobilized on the sensors surface. The spotted GMR chip was incubated for 24 h at 4 °C under a relative humidity of ~90%. After being rinsed with immunoassay stabilizer (SC01-1000, SurModics) three times to remove unbound capture antibody, the chip was further washed with PBST (0.02% tween 20 in PBS) and DI water, and was dried by nitrogen gas. A reaction well made of polymethyl methacrylate (PMMA) was attached onto chip surface. The reaction well can help to load a maximal liquid volume of 100 μL on sensor array area. A blocking buffer (1% BSA

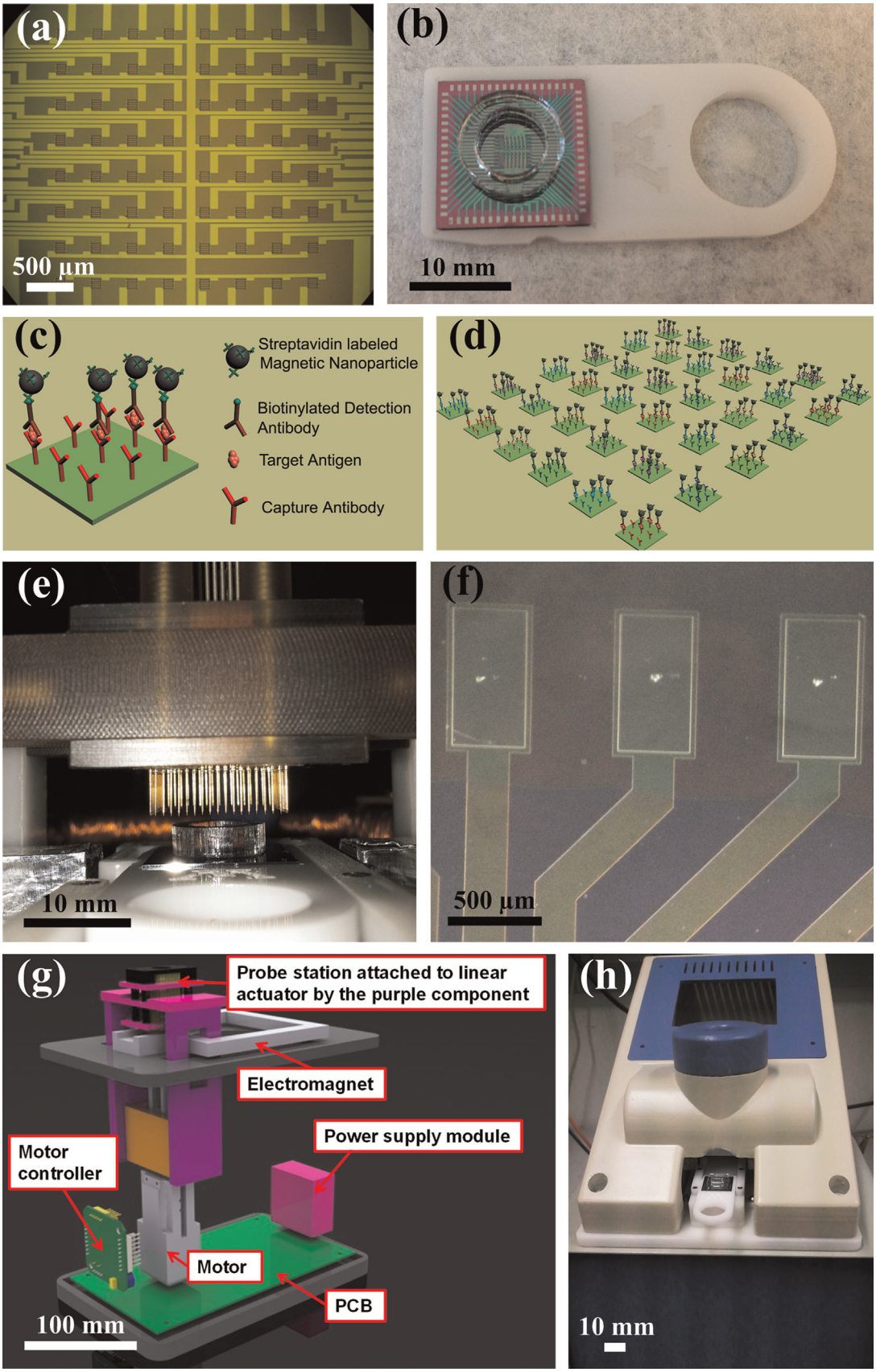

Fig. 1. (a) Photograph of the 64 (8 × 8 array) sensors on one chip. (b) Photograph of one GMR chip with the size of 16 mm × 16 mm and one reaction-well attached chip on the chip holder. (c) Schematic representation of sandwich assay on one GMR sensor. (d) Schematic drawing of the multiplex protein array on one chip. (e) Photograph of Pin array aligning and moving close with the electrode pads of the GMR chip. (f) The marks made by compressed pins on electrode pads. (g) Schematic design of the probe station. (h) Photograph of lab-based probe station system.

in PBST, 100 μL) was loaded into the reaction well. The chip was blocked for 1 h at room temperature to reduce nonspecific surface binding sites, and then the blocking buffer was aspirated and the chip was rinsed three times with PBST buffer. Samples consisted of multiple target proteins were prepared by mixing the three analytes (PAPP-A, PCSK9, and ST2 antigens) to the desired concentrations in PBS. 100 μL of this sample solution was pipetted into the reaction well and incubated for 1 h at room temperature, so that all of the sensors on the chip were exposed to the same multiple proteins solution and different capture antibodies on different sensors can bind to their antigens. Subsequently, the chip was rinsed three times with PBST buffer. The three PAPP-A, PCSK9, and ST2 detection antibodies was mixed in PBS to prepare the detection solution, and each antibody was finally at a concentration of 5 μg/mL. The solution (100 μL) was incubated in the reaction well for 1 h at room temperature, and then the chip was washed with PBST and dried by nitrogen gas.

2.5. Analyte quantification and magnetic label

The dry/wet transitions on sensor surface occasionally shifted the baseline slightly, and this would interfere with the detection signal. Thus, 30 μL of PBS solution was pipetted into the reaction well. After 5 min incubation, the chip was connected to the probe detection system (Wang et al., 2014a, 2014b), which was capable of ultrasensitive, multiplexed, real-time signal readout. After running for 10 min, 30 μL of magnetic nanoparticles (MNPs) solution was added. The absolute signal level before the addition of MNPs was taken to be zero. The MNPs solution was incubated without stirring for the next 30 min at room temperature. The signal levels at the end of this 30 min were taken as the final results of the assay. The MNPs with a size of 50 nm were purchased from Miltenyi Biotech Inc. (catalog no. 130-048-102), and their surface is functionalized with streptavidin. These MNPs are dispersed and colloidally stable, so they do not aggregate and settle on sensor surface. As the signal measurement was finished, the GMR chip was taken out and washed with DI water to remove any unbound MNPs, followed by being dried by nitrogen gas. Then the chip was coated with 5 nm Au film and further imaged by Field Emission Scanning Electron Microscopy (FESEM, JEOL 6500).

2.6. Detection system setup and signal measurement

Wire bonding is the most common way to package sensor chips. A new lab-based packaging system which is much more convenient and also could be used for handheld setting had been developed here instead. The connection between the GMR sensor and the circuit board is accomplished by the probe station holding a pin array, as shown in Fig. 1(e). One pin consists of one probe and one socket, which is designed for bare and loaded board testing. With extremely small sizes of diameter (0.56 mm at the thickest part) and length (32.26 mm), testing pins from QA Technology perfectly fit the current sensor design. According to the layout design, a four-layer probe holder was manufactured to fix and arrange the positions of the 68-pin array. Each pin will be aligned to one electrode pad which is connected to one sensor. Good electrical contact can be achieved by compressing the pins into 2/3 stroke and the probe holder keeps all pins stay straight and vertical during the process. As shown in Fig. 1(g), the motion (vertically up or down) of the probe holder is controlled by a stepper motor and a one-axis actuator. In Fig. 1(f), the alignment results could be observed from the marks made by the compressed pins on the contact pads through the optical microscope. The probe station (the photo is shown in Fig. 1(h)) is easy for users to operate in the laboratory, and the entire set-up process of each experiment is controlled by the computer and only takes less than 5 min. Unlike wire bonding, the probe station only consumes chips themselves without disposing the package sockets and 1,000,000 cycles of the probe lifetime is competitive when it is compared with fragile wires during the transport and operation. Implementing probe station also avoids any contamination from wire bonding.

In the detection system, National Instruments USB-6289 Data Acquisition (DAQ) module works as an analog output signal generator and an input signal digitizer. Two analog output channels are needed to generate two alternate currents for circuit and magnetic coil, respectively, and one digital-to-analog converter (DAC) input channel is used to gathered final signals with 18 bit and 500 kS/s. The digitization of the analog input channel has absolute accuracy at full scale (-0.1 V–0.1 V) which can reach 28 μV and its highest sensitivity is 0.8 μV with the built-in low pass filter. Another multiple analog low pass filter is designed in the circuit board to further suppress most noise sources, especially from the output channel. The frequency and phase jitter can be avoided effectively since the input and output channels of DAQ shares the same clock source. Multiplexers ADG1606i is used to address 64 GMR sensors and each multiplexer has 16 bi-directional single channels. 4-bit binary address lines control the bi-directional channel switching through the digital output channel of DAQ. Small useful signals can be amplified and detected since a Wheatstone bridge is added in the PCB to cancel out the analog background. The reference resistor has been adjusted to match the resistance of GMR sensors. An instrumentation amplifier INA163 is used to amplify the canceled signal. A potentiometer is added to adjust the gain value which optimizes the SNR and fit the range of DAQ input channel (Wang et al., 2014a, 2014b).

The reaction well attached on the GMR sensor is preloaded with 30 μL PBS solution to wet the sensor surface. The probes fixed in the probe station are driven by a programmed stepper motor to descend to the electrodes on the chip after the chip holder with the chip is inserted. Since all probes and electrodes are aligned, the connections are well and stable once working strokes of the probes are made by the motion of the probe station. The sensing current of 1000 Hz through the sensor is 30 μA, and the external in-plane field at 50 Hz applied along the short axis of the stripe sensor is 30 Oe. The time-domain signal is collected from the DAQ and then a Fast Fourier Transform would be done to trace the amplitude at mixing tones (1000 ± 50 Hz). The mixing tones are the primary signals in the real-time measurement and they can abstain from the 1/f fluctuation and the interference. The measurement is designed to sweep from one sensor to the next continuously and within one second the amplitude and phase from the currently measured sensor would be gathered. 30 μL of MNPs solution is added in the reaction well after 10 minutes background running. The dynamic particle binding process normally takes 5 min and simultaneously the trend of the signal increasing is observed by the real-time measurement system.

3. Results and discussion

3.1. GMR biosensor and detection principle

A structure of the multilayer thin films for the spin-valve type GMR sensor was applied in this work (Fig. S1). The free layer in the GMR thin film was composed of NiFe and CoFe bi-layers. The CoFe layer was introduced to prevent the interdiffusion between permalloy and copper since the lattice constants for these two were quite close (Nicholson et al., 1997). The 8×8 symmetrical array design would be propitious for quick and automatic spotting with antibodies on sensor surface. Each sensor was accordingly connected to contact pads on the periphery of the chip via contact

lines. The sensors could be connected to the probe system through the contact pads (Wang et al., 2014a, 2014b). The experiment showed that GMR sensors would be corroded by buffer solution without protective layer, and the sensor also experienced some degree of AC current leakage with only a thin SiO_2 layer on surface. Herein, bilayer of 20 nm Al_2O_3 and 20 nm SiO_2 was employed for the surface passivation. Additionally, Si_3N_4 layer has also been reported to be durable passivation for GMR sensors (Millen et al., 2008).

The principle of the GMR bio-sensing for this work is illustrated in supplementary material (Fig. S3). The direction of the pinned layer for the spin valve is in-plane and perpendicular to the sensor strips, and the easy axis of the free layer is parallel to the strip due to the shape anisotropy. In the absence of an applied AC field, GMR sensors have median magnetoresistance (MR) and they work at the most sensitive region. When magnetic nanoparticle labels are bound to the sensor surface, they can be magnetized as dipoles, and their introduced stray fields may reduce the AC field. The change in the AC field leads to a change in the MR of the sensor, which can be measured and read out as the primary detection signal using the probe platform.

Sandwich assay format was used in this study. Its detection architecture on GMR sensor surface is schematically illustrated in Fig. 1(c). Capture antibody was immobilized on the sensor surface, and then target antigen and biotinylated detection antibody was successively added and bound. Finally magnetic labels (streptavidin coated MNPs) were bound to sensor surface via the biotin–streptavidin interaction. As shown in Fig. 1(d), many of proteins binding experiments could be run in one shot on one GMR chip as different antibodies were captured on different sensor surface. Currently, this prototype GMR biochip is able to simultaneously monitor up to 64 proteins in principle. It is also worth mentioning that this is not the limit of detection capability for one GMR chip, and the GMR sensors could be scaled to over 100,000 sensors per cm^2 (Gaster et al., 2011). Therefore, further development of the bio-sensing could enable it to be a robust high-throughput screening technology.

3.2. Multi-analyte detection

Before GMR sandwich assays were performed, the proteins had been tested in a similar experimental protocol on silicon wafer surface. The fluorescence detection results (Fig. S4) indicate that the concentration of biotinylated detection antibody plays an important role in this assay, and the optimal concentration is 5 μg/mL. Thus, 5 μg/mL of the detection antibody is used in the GMR assay. The fluorescence sandwich demonstration of PAPP-A antigen (Fig. S5) shows that the fluorescence intensity of printed spots is getting stronger as the concentration of PAPP-A antigen rises up. From the fluorescence images, these spots are uniform and the background signal is very low. It further proves that the experimental protocol for the biological binding part works well.

The typical real-time binding curves (signal vs. time) for PAPP-A assay are shown in Fig. 2a. Beginning at $t=10$ min, the signals for

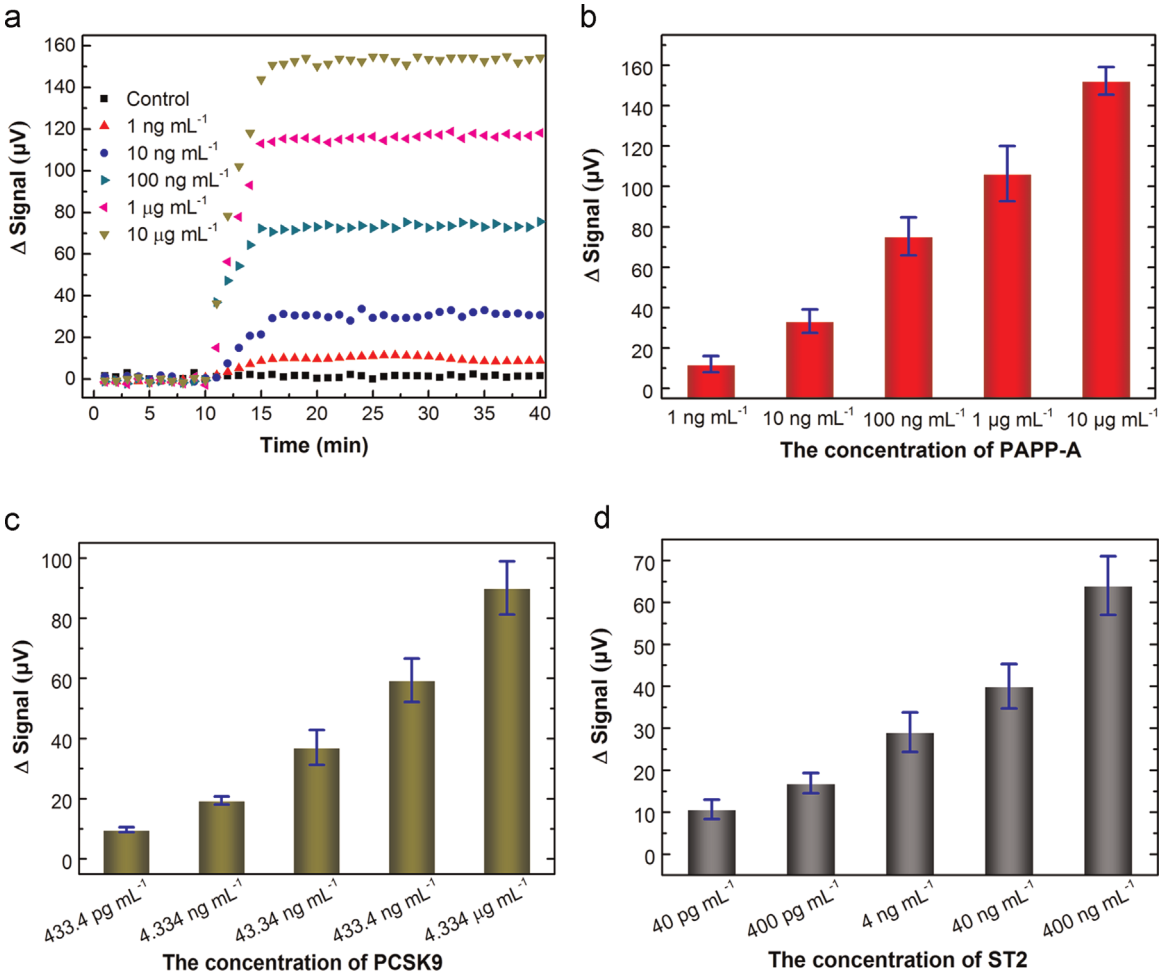

Fig. 2. (a) Typical binding curves in real time and (b) Average final signals (with standard deviation) for PAPP-A antigen. (c) The detection signals (with standard deviation) for PCSK9 antigen. (d) The detection signals (with standard deviation) for ST2 antigen.

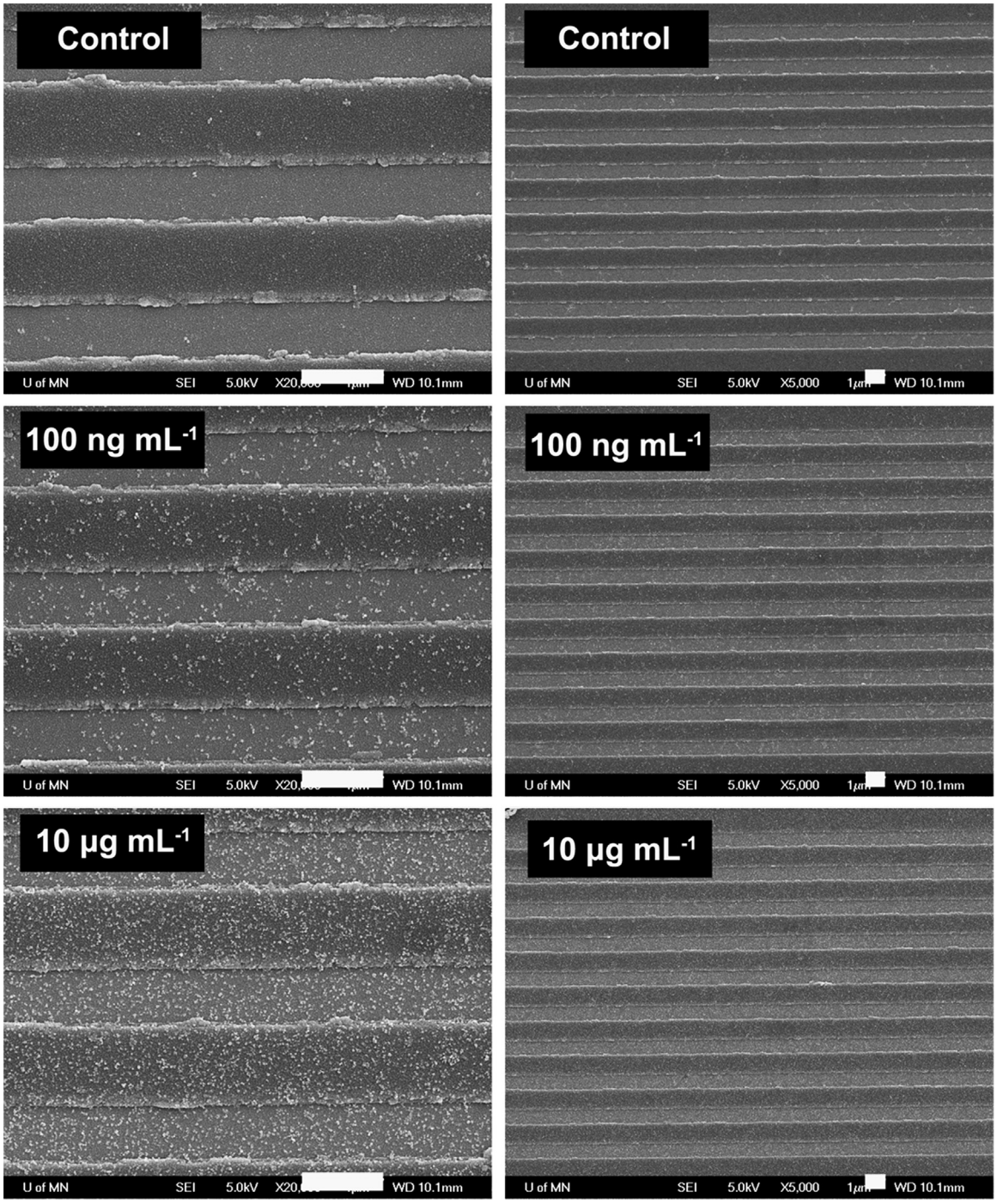

Fig. 3. SEM images of MNPs bound on GMR sensor surface after protein assay. The two upper images show the control sensor surface covered by BSA. Other four images are for PAPP-A assay with different concentrations. All the scale bars are 1 μm.

various PAPP-A concentrations show a rise, which reflect real-time binding of MNPs to sensor surface. As expected, the signal does not show an obvious rise for the control sensor which has been blocked with BSA, indicating rarely non-specifically binding of MNPs to the sensor surface. These rising signals saturate within 5–10 min, implying that MNPs binding has reached equilibrium on sensor surface. Higher saturated signal level is detected for higher concentration of PAPP-A antigen. Similar binding curves are also observed for PCSK9 and ST2 antigen assays. The final detection signal is calculated by subtracting background signal from saturated signal. Their final average signals for various PAPP-A concentrations are presented in Fig. 2b. The limit of detection (LOD) of this assay for PAPP-A is 1 ng/mL, and the magnitude of dynamic range using GMR sensing technology reaches up to 4 orders of magnitude (1 ng/mL–10 μg/mL). The average signals for 1 ng/mL PAPP-A is about 12 μV, and it goes up with an increase in PAPP-A concentration. The highest signal reaches 152.3 μV for 10 μg/mL PAPP-A.

A further investigation on sensor surface with bound MNPs was implemented. The SEM results (Fig. 3) reveal that very few MNPs were bound on control sensor surface, which is in accordance with the control signal result. In contrast, the bound numbers for 100 ng/mL and 10 μg/mL PAPP-A sample are up to roughly 50/μm^2 and 135/μm^2 respectively. For GMR bio-sensing technology, the

Table 1
Comparison of ST2 detection based on various methods.

Methods	Dynamic range (ng/mL)	Limit of detection (ng/mL)	Reference
Presage ST2 assay	3.1 – 200	1.8	Mueller and Dieplinger (2013)
MBL ST2 assay	0.1875–12	0.1875	Mueller et al. (2012)
R&D ST2 assay	0.03125–2	0.03125	Mueller et al. (2012)
GMR nanodevice	0.04–400	0.04	This work

final output signal has a relationship with the bound number of MNPs (Schotter et al., 2004; Mulvaney et al., 2007). Consequently, for detecting a biological or chemical agent using GMR biosensor, it is critical to build a model that the number of bound MNPs is dependent on the added amount of the biological target.

As shown in Fig. 2c and d, the dynamic ranges for PCSK9 and ST2 assays are also up to 4 orders of magnitude, and their LOD are 433.4 pg/mL and 40 pg/mL respectively. ST2 detection based on various methods is summarized in Table 1. It shows that the three commercially available assay kits for ST2 have different detection limits. Previous report (Mueller et al., 2012) indicates that the ST2 plasma concentrations for the same group of patients obtained with the three assays were not equal to each other. The reasons are most probably different standards and/or different antibodies, and perhaps also different reagents and buffers. Comparing the proposed GMR biosensor with the R&D ST2 assay is probably more reasonable because the proteins and reagents are obtained from R&D Systems, Inc. The GMR biosensor possesses comparable detection limit for the detection of ST2 with respect to the R&D ST2 assay, and it has much wider detection orders in dynamic range.

3.3. Magnetic labels and selection strategy

As an indispensible part in GMR biosensor platform, magnetic labels are significantly vital to the detection capability. Therefore, choosing the appropriate magnetic labels has great implication for developing this sensing technology. At present, commercially available magnetic labels are usually functionalized magnetic micro- or nano-particles. As compared with MNPs, magnetic microparticles are undesirable because they would hinder high-density binding across sensor surface and have a larger adverse effect on the final signal when non-specific binding event occurs. Nanoparticles with much smaller size have a stronger Brownian motion and it contributes to the diffusion and binding processes. Superparamagnetic property is also one of unparalleled profits from MNPs. However, small-sized MNPs usually possess small magnetic moment, which may result in low detection signal compared with large-sized MNPs (Jing et al., 2009). Therefore, in order to determine the optimal MNPs in GMR biosensing system, a comprehensive consideration and even a set of experiments need to be performed. The magnetic labels used in this work are MNPs with a size of 50 nm (its magnetic hysteresis loop is shown in Fig. S6). It appears that almost no coercivity is observed, confirming its superparamagnetic property. The magnetic saturation values (Ms) per particle for the MNPs is 8.1×10^{-15} emu. The surface charge (-11 mV at pH 7.4 for ζ potenial) and polymer (dextran) coating enable the MNPs to be colloidally stable. So the MNPs can avoid aggregating and settling which might generate non-specific binding signal.

Comparison of proteins detection using 20 nm colloidal MNPs and the 50 nm MNPs is presented in Fig. 4. The signals for PAPP-A and ST2 using the 20 nm MNPs are both much lower than that produced by the 50 nm MNPs. The Ms per particle for the 20 nm MNPs is 7.8×10^{-16} emu (data not shown), an order of magnitude lower than the Ms value for the 50 nm MNPs. For GMR biosensor, MNPs with high magnetic moment are desired overall.

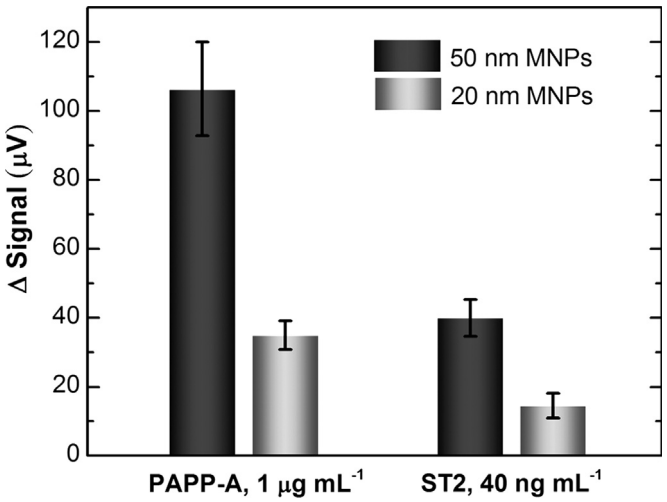

Fig. 4. Comparison of proteins detection using 20 nm MNPs (Ocean NanoTech, SHS-20) and 50 nm MNPs (Miltenyi Biotech, MACS 130-048-102).

3.4. Detection of analytes in Blood serum

To determine whether the signals detected in serum would be different from buffer, protein analytes were spiked in healthy human serum. Their comparisons are shown in Fig. 5. The detection results for 4.334 ng/mL PCSK9 show a difference in buffer and serum environment since serum PCSK9 level can range from 12 to 225 ng/mL (Cui et al., 2010; Dubuc et al., 2010). Meanwhile, the results of PAPP-A and ST2 detections in buffer and serum do not differ statistically, indicating that the GMR assay works with same efficiency in complex biological environment as it does in buffer. This is of vital importance for fulfilling the clinical application of the GMR biosensor system.

4. Conclusion

By virtue of its inherent advantages, GMR biosensor as a robust analytical tool for diagnostic testing had emerged recently. This work presents herein a lab-based real-time biomolecule detection system by the sensing scheme between GMR sensors and MNPs. The GMR chip with 64 sensor array is connected into the detection

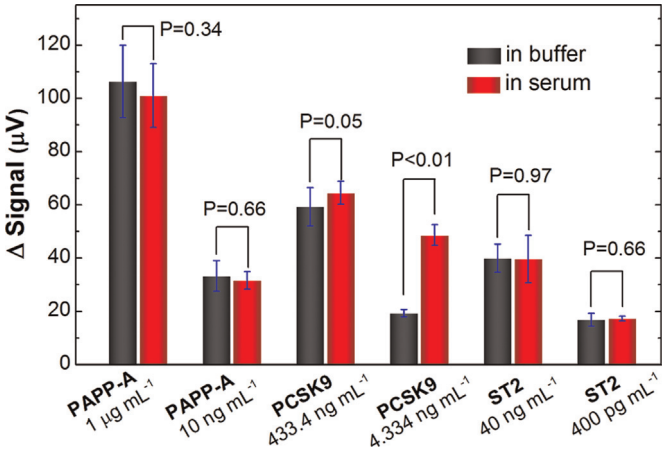

Fig. 5. Comparison of proteins detection in buffer and biological environment (spiked proteins in human serum). Columns: mean; bars: standard deviation; $p > 0.05$ means they showed no statistically significant difference; $p < 0.01$ means they showed statistically significant difference.

circuit through the probe station, and the sensors can be independently and simultaneously monitored. Based on sandwich assay format, three protein biomarkers had been measured and analysed by the proposed GMR biosensor system which had the merits of high sensitivity, high-level multiplex capability, and real-time signal readout. Four orders of magnitude dynamic range for PAPP-A, PCSK9, and ST2 antigens, had been achieved, as well as a detect limit of 40 pg/mL for ST2. Furthermore, the possibility of analysing biomarkers in blood serum was tested. Also the new probe station system free of wire bonding makes the lab-on-a-chip experiments more convenient and quicker, which shows promising application prospect in real clinical settings.

Acknowledgments

This work was partially supported by the Office for Technology Commercialization and the Institute of Engineering in Medicine (University of Minnesota). Parts of this work were carried out in the Characterization Facility, University of Minnesota, which receives partial support from National Science Foundation through the MRSEC program. We are grateful of the useful discussion with Dr. Michael Anderson from R&D Systems. We also thank R&D Systems, Inc. (USA) for providing the protein samples. Joseph Coffey, Dingyi Li, Jay Beversdorf, Ismail Akharas and April Ruggles from the University of Minnesota also partially contributed to the mechanical parts of the system through a Mechanical Engineering Department senior design project.

Appendix A. Supplementary Information

Supplementary data associated with this article can be found in the online version at http://dx.doi.org/10.1016/j.bios.2015.03.011.

References

Baselt, D.R., Lee, G.U., Natesan, M., Metzger, S.W., Sheehan, P.E., Colton, R.J., 1998. Biosens. Bioelectron. 13, 731–739.
Bonaca, M.P., Scirica, B.M., Sabatine, M.S., Jarolim, P., Murphy, S.A., Chamberlin, J.S., Rhodes, D.W., Southwick, P.C., Braunwald, E., Morrow, D.A., 2012. J. Am. Coll. Cardiol. 60, 332–338.
Chan, K., Ng, M., Stocker, R., 2011. Clin. Sci. 120, 493–504.
Cui, Q., Ju, X., Yang, T., Zhang, M., Tang, W., Chen, Q., Hu, Y., Haas, J.V., Troutt, J.S., Pickard, R.T., 2010. Atherosclerosis 213, 632–636.
Dubuc, G., Tremblay, M., Paré, G., Jacques, H., Hamelin, J., Benjannet, S., Boulet, L., Genest, J., Bernier, L., Seidah, N.G., 2010. J. Lipid Res. 51, 140–149.
Fragoso, A., Latta, D., Laboria, N., von Germar, F., Hansen-Hagge, T.E., Kemmner, W., Gärtner, C., Klemm, R., Drese, K.S., O'Sullivan, C.K., 2011. Lab on a Chip 11, 625–631.
Gaster, R.S., Xu, L., Han, S.-J., Wilson, R.J., Hall, D.A., Osterfeld, S.J., Yu, H., Wang, S.X., 2011. Nat. Nanotechnol. 6, 314–320.
Gaster, R.S., Hall, D.A., Nielsen, C.H., Osterfeld, S.J., Yu, H., Mach, K.E., Wilson, R.J., Murmann, B., Liao, J.C., Gambhir, S.S., 2009. Nat. Med. 15, 1327–1332.
Gordon, J., Michel, G., 2012. Clin. Chem. 58 (4), 690–698, and references in section of Giant Magnetoresistive Sensor Technology.
Graham, D.L., Ferreira, H.A., Freitas, P.P., 2004. Trends Biotechnol. 22, 455–462.
Homola, J., Vaisocherová, H., Dostálek, J., Piliarik, M., 2005. Methods 37, 26–36.
Hu, M., Yan, J., He, Y., Lu, H., Weng, L., Song, S., Fan, C., Wang, L., 2009. ACS Nano 4, 488–494.
Huijgen, R., Boekholdt, S.M., Arsenault, B.J., Bao, W., Davaine, J.-M., Tabet, F., Petrides, F., Rye, K.-A., DeMicco, D.A., Barter, P.J., 2012. J. Am. Coll. Cardiol. 59, 1778–1784.
Ivanov, K., Kolev, N., Tonev, A., Nikolova, G., Krasnaliev, I., Softova, E., Toncbev, A., 2009. Hepato-gastroenterology 56, 94–98.
Jing, Y., He, S., Kline, T., Xu, Y. Wang., J.-P. 2009. Proceeding of 31st Annual International Conference of the IEEE EMBS. pp. 4483–4486.
Li, Y., Zhou, C., Zhou, X., Song, L., Hui, R., 2012. Clin. Chim. Acta.
Li, Y., Srinivasan, B., Jing, Y., Yao, X., Hugger, M.A., Wang, J.-P., Xing, C., 2010. J. Am. Chem. Soci. 132, 4388–4392.
Madu, C.O., Lu, Y., 2010. J. Cancer 1, 150.
Martins, V., Cardoso, F., Germano, J., Cardoso, S., Sousa, L., Piedade, M., Freitas, P., Fonseca, L., 2009. Biosens. Bioelectron. 24, 2690–2695.
Millen, R.L., Nordling, J., Bullen, H.A., Porter, M.D., Tondra, M., Granger, M.C., 2008. Anal. Chem. 80, 7940–7946.
Mueller, T., Dieplinger, B., 2013. Expert Rev. Mol. Diagn. 13, 13–30.
Mueller, T., Zimmermann, M., Dieplinger, B., Ankersmit, H.J., Haltmayer, M., 2012. Clin. Chim. Acta 413, 1493–1494.
Mulvaney, S., Cole, C., Kniller, M., Malito, M., Tamanaha, C., Rife, J., Stanton, M., Whitman, L., 2007. Biosens. Bioelectron. 23, 191–200.
Murphy, B.M., He, X., Dandy, D., Henry, C.S., 2008. Anal. Chem. 80, 444–450.
Nicholson, D., Butler, W., Shelton, W., Wang, Y., Zhang, X.-G., Stocks, G., MacLaren, J., 1997. J. Appl. Phys. 81, 4023–4025.
Qureshi, A., Niazi, J.H., Kallempudi, S., Gurbuz, Y., 2010. Biosens. Bioelectron. 25, 2318–2323.
Rehman, S.U., Mueller, T., Januzzi, J.L., 2008. J. Am. Coll. Cardiol. 52, 1458–1465.
Rife, J.C., Miller, M.M., Sheehan, P.E., Tamanaha, C.R., Tondra, M., Whitman, L.J., 2003. Sensor. Actuat. A-Phys 107, 209–218.
Roda, A., Mirasoli, M., Dolci, L.S., Buragina, A., Bonvicini, F., Simoni, P., Guardigli, M., 2011. Anal. Chem. 83, 3178–3185.
S. Parkin, X. Jiang, C. Kaiser, A. Panchula, K. Roche and M. Samant. 2003. Proceedings of the IEEE, 91, 661–680.
Schotter, J., Kamp, P.-B., Becker, A., Pühler, A., Reiss, G., Brückl, H., 2004. Biosens. Bioelectron. 19, 1149–1156.
Simon, L., Gauvin, F., Amre, D.K., Saint-Louis, P., Lacroix, J., 2004. Clin. Infect. Dis. 39, 206–217.
Srinivasan, B., Li, Y., Jing, Y., Xu, Y., Yao, X., Xing, C., Wang, J.-P., 2009. Angew. Chem. Int. Ed. 48, 2764–2767.
Tarzami, S.T., 2011. Int. J. Clin. Exp. Med. 4, 74.
Tsang, C.H., Fontana, R., Lin, T., Heim, D.E., Gurney, B.A., Williams, M., 1998. IBM J. Res. Dev. 42, 103–116.
Vasan, R.S., 2006. Circulation 113, 2335–2362.
Wang, W., Wang, Y., Tu, L., Klein, T., Feng, Y., Wang, J.-P., 2013. IEEE Trans. Magn. 49, 296–299.
Wang, W., Wang, Y., Tu, L., Feng, Y., Klein, T., Wang, J., 2014b. Sci. Rep. 4, 5716.
Wang, W., Wang, Y., Tu, L., Klein, T., Feng, Y., Li, Q., Wang, J.-P., 2014a. Anal. Chem. 86, 3712–3716.
Weinberg, E.O., Shimpo, M., Hurwitz, S., Tominaga, S.-i, Rouleau, J.-L., Lee, R.T., 2003. Circulation 107, 721–726.
Wilson, M.S., Nie, W., 2006. Anal. Chem. 78, 6476–6483.
Zhang, Z., Bast, R.C., Yu, Y., Li, J., Sokoll, L.J., Rai, A.J., Rosenzweig, J.M., Cameron, B., Wang, Y.Y., Meng, X.-Y., 2004. Cancer Res. 64, 5882–5890.
Zheng, G., Patolsky, F., Cui, Y., Wang, W.U., Lieber, C.M., 2005. Nat. Biotechnol. 23, 1294–1301.
Zhi, X., Liu, Q., Zhang, X., Zhang, Y., Feng, J., Cui, D., 2012. Lab on a Chip 12, 741–745.